agronomy

MDPI

*Article*

# Polyploid Miscanthus Lutarioriparius: A Sustainable and Scalable Biomass Feedstock for Cellulose Nanocrystal Preparation in Biorefinery

**Sheng Wang [1], Zili Yi [1,2,3], Yasir Iqbal [1,2,3], Zhiyong Chen [1,2,3], Shuai Xue [1,2,3], Tongcheng Fu [1,2,3] and Meng Li [1,2,3,*]**

1 Hunan Provincial Key Laboratory of Crop Germplasm Innovation and Utilization, College of Bioscience & Biotechnology, Hunan Agricultural University, Changsha 410128, China; 179683260@stu.hunau.edu.cn (S.W.); yizili@hunau.net (Z.Y.); yasir.iqbal1986@googlemail.com (Y.I.); zhiyongchen@hunau.edu.cn (Z.C.); xue_shuai@hunau.edu.cn (S.X.); futongcheng@hotmail.com (T.F.)
2 Hunan Branch, National Energy R&D Center for Non-Food Biomass, Hunan Agricultural University, Changsha 410128, China
3 Hunan Engineering Laboratory of Miscanthus Ecological Applications, College of Bioscience & Biotechnology, Hunan Agricultural University, Changsha 410128, China
* Correspondence: mengli@hunau.edu.cn

**Abstract:** In this study, polyploid *Miscanthus lutarioriparius* (PML) was introduced as a new sustainable and scalable source for cellulose nanocrystal (CNC). The agronomic traits of PML were significantly different from *Miscanthus* × *giganteus* (MG), but their chemical components and physical features were similar. Notably, a remarkable co-extraction of hemicellulose, lignin and ash and non-crystalline cellulose was observed during crude cellulose isolation from PML than it from MG by modified alkaline peroxide pretreatment. In addition, subjecting crude cellulose of PML and MG biomass to sulfuric acid hydrolysis provided high-quality CNC. The analysis of particle size distribution, zeta potential, crystalline index, the degree of polymerization, SEM and yield potential suggested that the CNC extracted from PML showed higher stability, processability and productivity than that from MG. Therefore, it provides a new theoretical basis for the applications of CNC prepared by PML and MG. The results also revealed potential genetic approaches for *Miscanthus* spp. to enhance biomass and CNC yield.

**Keywords:** modified alkaline peroxide pretreatment; biomass feedstock agronomic traits; crude cellulose; cellulose nanocrystals

check for updates

**Citation:** Wang, S.; Yi, Z.; Iqbal, Y.; Chen, Z.; Xue, S.; Fu, T.; Li, M. Polyploid Miscanthus Lutarioriparius: A Sustainable and Scalable Biomass Feedstock for Cellulose Nanocrystal Preparation in Biorefinery. *Agronomy* **2022**, *12*, 1057. https://doi.org/10.3390/agronomy12051057

Academic Editor: Stefano Amaducci

Received: 29 March 2022
Accepted: 26 April 2022
Published: 28 April 2022



## 1. Introduction

Lignocellulose is a promising feedstock for biorefinery, which mainly consists of ligin, hemicellulose and cellulose. The chemical components of lignocellulosic biomass make them a substrate of enormous biotechnological value [1]. Several of the polysaccharides possessing interesting physical and biological properties have been applied in biotechnology products or are presently being widely investigated (i.e., hyaluronic acid, alginate, chitosan) [2]. With the development of cellulose research, cellulose nanocrystal (CNC) separated from lignocellulose has emerged as a promising material and a major focus in nanomaterial research [3].

Cellulose nanocrystal is a polymer produced by the hydrolysis of cellulose. CNCs are rod-like particles with a highly crystalline structure, high aspect ratio, large surface area, unique tensile strength (0.8–10 GPa), low density and high Young's modulus (100–170 GPa) [3]. Advantages in the use of CNC are related not only to their useful, unsurpassed, physical features, but also to their biodegradability, renewability, sustainability, abundance and high biocompatibility. Some authors have proposed that nanotechnology will change our lives in profound ways, allowing engineers to devise more efficient ways of meeting human needs [4,5]. It is believed that nanotechnology has the potential to completely change lignocellulose products and the biomass "industry" through improvements in the products and by designing new applications of biomass-derived materials with different properties [6,7]. CNC is posited as being a high potential material for the multi-industries of food [8], packaging [9], (bio)sensors [10], and medicine [11].

Various materials with a high content of cellulose could be used to prepare CNC, such as wood [12], bamboo [13], crop residue [14], and bagasse [15]. However, the geometrical characteristics of CNC (i.e., shape, particle size, aldehyde and carboxyl groups) would significantly vary according to different raw materials and reaction conditions [16]. Although woody materials are an optimal feedstock for CNC production, such reserves are steadily declining [17]. The continuous supply of woody materials for the CNC industry might not be environmentally friendly, and may not be feasible in the coming decades. Therefore, the shortage of ideal feedstock is a bottleneck for the industrial application of CNC.

*Miscanthus lutarioriparius* is a high-yield perennial lignocellulosic crop endemic to China and is widely distributed along Hunan, Hubei, Zhejiang, Anhui, Jiangsu, Jiangxi, Henan, Shanghai province. It is a promising second-generation energy crop with high stress resistance, a wide propagation range, stable genetic properties, and is widely grown as a marginal crop [18]. It has been evaluated that *M. lutarioriparius* could produce an annual biomass of 28.37 ton/ha in alkaline land [19]. Meanwhile, *M. lutarioriparius* is regarded as a good biomass feedstock, because its stem has a high content of lignocellulose and a low content of ash [20]. Several processes and products have been reported that utilize *M. lutarioriparius* as a raw material for industrial applications. These include bioenergy [21], paper making [19] and building materials [22]. In addition, prior studies found that polyploid *M. lutarioriparia* (PML) has the characteristics of thick stems, high biomass yield, and tolerance to floods and droughts, and so has greater development potential than diploids [4,22].

In *Miscanthus* spp., there exists another high biomass potential polyploidy called *Miscanthus* × *giganteus* (MG) [23]. Experimental bases for studying the biomass potential of triploid MG in northern Europe have been established successively in Denmark, Germany, Ireland, and the United Kingdom [24]. In 1993, Greef and Deuter speculated that MG was a triploid and was hybridized by *M. sacchariflorus* (tetraploid) and *M. sinensis* (diploid). MG is now a widely cultivated perennial energy crop in Europe which is used for electricity generation and bioethanol production [23,24]. However, the CNC feedstock potentials of both MG and PML have not been evaluated yet. Considering that perennial energy grass is a resource for biorefinery, it is necessary to assess the biomass potentials of MG and PML for CNC production. Therefore, the objectives of this study are (i) to investigate the differences in agronomic properties, (ii) the physical properties (i.e., Crystalline, degree of polymerization) between MG and PML, and (iii) to explore their potentials for preparing CNC.

## 2. Materials and Methods

### *2.1. Sampling and Measurements*

The study site is located at "The Nursery of *Miscanthus* Germpalsms" in Hunan Agricultural University (113°4′50.12400″ E, 28°11′5.67600″ N). In 2020, nine plants of PML and MG were grown in plots (1.5 m × 1.5 m) arranged in a randomized complete block design, with 11 replicates. Aboveground biomass in each plot was harvested manually and weighed to determine dry biomass weight (DBW), panicle height (PH), stem number (SN), stem diameter (SD), moisture content (MC), leaf length (LL), leaf width (LW), node number (NN) and leaf/stem ratio (L/S). The definitions of the characteristics are as follows. DBW: The dry weight per plant, measured using an electronic scale and expressed in kg. PH: The distance from the ground to the top of the panicle, expressed in cm. SN: The number of stems of the plant. SD: The diameter of the middle of the last segment of the stem, measured using vernier calipers and expressed in cm. MC: The difference between the weight of the plant at the time of sampling and the weight of the plant after drying, expressed as a percentage. LL: The length from leaf base to leaf tip, expressed in cm. LW: The length at the widest part of the leaf, expressed in cm. NN: The number of internodes of plant. L/S: The ratio of leaf weight (g) to stem weight (g) per plant. All samples were dried under 90 °C for 3 days. Dried samples were grounded to powder, and then sieved through a combined −80 mesh (0.180 mm × 0.180 mm) screen. Sieved dry samples as raw biomass were sealed in sealing bags and preserved at room temperature [25].

### 2.2. Flow Cytometry

First, 20 mg of sieved young leaves of the PML was added to 1 mL of Galbraith's buffer (containing 45 mmol/L $MgCl_2$, 30 mmol/L sodium citrate, and 20 mmol/L 3-(n-morphinol) propanulinic acid (pH 7.0). Then, 0.1% Triton X-100 and 50 µg/mL RNase were added, and the supernatant was discarded by centrifugation. The cell suspension was obtained by adding 500 µL Galbraith's buffer to the precipitate and shaking the mixture. The propidium iodide solution was dropped into the suspension until a final concentration of 50 µg/mL, and then the mixture was stained on ice for 30 min against light. At least 10,000 cells were collected from each sample to be tested, and this was repeated three times for each sample. The genome size was determined using Epics XL flow cytometry (Epics XL, Beckman Coulter Co., Ltd., Indianapolis, IN, USA). The fluorescence of the FL3 channel was collected by blue light excitation at 488 nm, and the emission fluorescence intensity of propidium iodide was detected using Tree Star FlowJo software [26].

### 2.3. Sample Pretreatment

Crude cellulose was extracted by the modified alkaline peroxide pretreatment according to Gabriel et al. [27] with minor modifications. In this study, we replaced 10% NaOH with 20% NaOH and 7.5% $H_2O_2$ with 20% $H_2O_2$. The first step of pretreatment was alkaline hydrolysis. Raw biomass was placed in sealed beaker 20% NaOH at the liquid to solid ratio 10:1, and oil-bathed at 100 °C for 1 h, 140 °C for 30 min, and 160 °C for 30 min to obtain the pulp. Obtained pulp was washed with distilled water to a neutral pH. For the next step, the pulp was washed by 20% $H_2O_2$ at liquid to solid ratio of 10:1, under 90 °C for 3 h to remove lignin. The solid and liquid were centrifugated to obtain precipitate. The precipitate was oven-dried and preserved with sealed plastic bags under room temperature. The yield of crude cellulose was calculated according to Equation (1).

$$CCY = (W_c \times (1 - m_c))/(W_b \times (1 - m_b)) \times 100\ [\%] \quad (1)$$

where, $CCY$ is crude cellulose yield (%); $W_c$ is the weight of crude cellulose (g); $m_c$ is the moisture content of crude cellulose (%); $W_b$ is the weight of biomass feedstock (g); and $m_b$ is the moisture content of biomass feedstock (%).

### 2.4. CNC Preparation

The CNC was prepared using a sulfuric acid hydrolysis method as introduced by Lunardi et al. [3] with minor modifications. The crude cellulose was hydrolyzed with 56% $H_2SO_4$, at a liquid to solid ratio of 20:1, under a temperature of 61 °C for 40 min to obtain the CNC. Upon expiration of the reaction time, the hydrolysis was stopped by fourfold dilution with distilled water and cooling of the suspension to room temperature. The hydrolyzed cellulose solution was dialyzed with periodic water replacement to achieve a neutral pH. The dialyzed cellulose solution was subjected to ultrasonic treatment with an ultrasonic disintegrator (KS-1000KDE, Kushan Jielimei Ultrasonic Instrument Co., Ltd., Kunshan, China) at 40 kHz, 300 W for 15 min, following filtration using 1 micrometer aperture filter paper. Filter liquor was transferred to a 150 mL volumetric flask and the volume was set with distilled water. A CNC solution of 1 mL was transferred from the volumetric flask to a beaker and diluted fiftyfold with distilled water, for the determination of CNC size. The remaining solution in the flask was frozen in a refrigerator at −20 °C for 12 h, then dried in a freezer dryer (LC-12N-80C, Shanghai Lichenbangxi Instrument Science Technology Co., Ltd., Shanghai, China). The freeze-dried CNC was preserved using sealed plastic bags. The yield of CNC was calculated according to Equation (2).

$$CNCY = W_n \ / \ (W_c \times (1 - m_c)) \times 100 \ [\%] \tag{2}$$

where, $CNCY$ is crude cellulose yield (%); $W_n$ is the weight of CNC (g);.$m_c$ is the moisture content of crude cellulose (%); and $W_c$ is the weight of crude cellulose (g).

### *2.5. Biomass Feedstock Chemical Contents Measurement*

Soluble contents of PML and MG were extracted from raw biomass and crude cellulose using 75% ethyl alcohol, and after six cycles, the value was found to be the difference between the weight of the biomass feedstock and the weight of the biomass feedstock after extraction. The soluble content was calculated according to Equation (3).

$$SC = (W_{ap} \times (1 - m_{ap}) \ / \ (W_b \times (1 - m_b)) \times 100 \ [\%] \tag{3}$$

where, $SC$ is soluble content (%); $W_{ap}$ is the weight of biomass feedstock or crude cellulose after extraction (g); $m_{ap}$ is the moisture content of biomass feedstock or crude cellulose (%); $W_b$ is the weight of biomass feedstock (g); and $m_b$ is the moisture content of biomass feedstock (%).

Ash content was determined using a muffle furnace (SX-4-10, Tianjin Taisite Instrument Co., Ltd., Tianjin, China) with 15 mL ceramic crucibles [28]. The ash content was calculated according to Equation (4).

$$AC = (W_{ar} - W_r) \ / \ (W_b \times (1 - m_b)) \times 100 \ [\%] \tag{4}$$

where, $AC$ is ash content (%); $W_{ar}$ is the weight of crucible after calcination (g); $W_r$ is the weight of crucible (g); $W_b$ is the weight of biomass feedstock (g); and $m_b$ is the moisture content of biomass feedstock (%).

A two-step sulfuric acid hydrolysis process was used to extract cellulose, hemicellulose and lignin [25]. Structural carbohydrates (i.e., glucose, xylose, and arabinose) were measured using an HPLC system (LC-40, SHIMADZU Co., Ltd., Kyoto, Japan) equipped with an Aminex HPX-87H chromatography column (300 mm × 7.8 mm, particle size 9 μm, Bio-Rad Laboratories, Hercules, CA, USA) and a refractive index detector (RID 20A, SHIMADZU Co., Ltd., Kyoto, Japan). The lignin content was measured using a UV-VIS spectrometer (A590, Aoyi Instrument Shanghai Co., Ltd., Shangha, China) and the same muffle furnace mentioned above. The cellulose content and hemicellulose content were calculated according to Equation (5).

$$Y = \frac{C \times e \times V \times X}{1000 \times W \times (1 - b) \times f} \times 100 \ [\%] \tag{5}$$

where, $Y$ is cellulose content (%) or hemicellulose content (%); $C$ is the concentration of fiber polysaccharides (mg/mL); $e$ is the mass conversion coefficient of polysaccharides into monosaccharides by dehydration; $V$ is the hydrolysate volume (mL); $X$ is the extraction residue rate (%); $W$ is the weight of sample (g); $b$ is the moisture content of sample (%); and $f$ is the recovery coefficient of chromatographic correction standard sample.

The lignin content is calculated according to Equation (6).

$$L = \frac{U \times V \times n \times X}{1000 \times \varepsilon \times W \times (1 - b)} + \frac{(W_L) \times X}{W \times (1 - b)} \times 100 \ [\%] \tag{6}$$

where $L$ is lignin content (%); $U$ is the absorbance of neutral hydrolysate at 320 nm; $e$ is the mass conversion coefficient of polysaccharides into monosaccharides by dehydration; $V$ is the hydrolysate volume (mL); $n$ is the dilution ratio of hydrolysate; $X$ is the extraction residue rate (%); $b$ is the moisture content of sample (%); $\varepsilon$ is the Light absorption rate of hydrolysate (L/(g·cm)); and $W_L$ is the weight of precipitation (g).

The purity is determined by the cellulose content of CNC.

### *2.6. CNC Physical Property Measurement*

The cellulose crystallinity index was detected with the X-ray diffraction (XRD) method using an X-ray diffractometer (XRD-6000, SHIMADZU Co., Ltd., Kyoto, Japan) [29]. The raw biomass power was laid on the glass sample holder and detected under plateau conditions. Ni-filtered Cu Ka radiation (k = 0.15406 nm) was generated at a voltage of 40 kV and a current of 30 mA and scanned at a speed of 5°/min from 10° to 35°. The *Crl* was estimated using the intensity of the 200 peak ($I_{200}$, h = 22.5°) and the intensity at the minimum point between the 200 and 110 peaks ($I_{am}$, h = 18.5°).

$$CrI = (I_{200} - I_{am})/I_{200} \times 100\ [\%] \tag{7}$$

where *CrI* is the cellulose crystallinity index; $I_{200}$ is the intensity of the peak at 22.5°; and $I_{am}$ is the intensity of the minimum between the 200 and 110 peaks at 18.5°.

The degree of polymerization (DP) was determined with the Ubbelohde Viscosity Test [30]. Copper ammonia solution (double hydroxide ethylenediamine copper solution:distilled water ($V/V$) = 1:1) was used to determine the DP. Since the viscosity of the copper ammonia solution is easily affected by temperature, the value of the measured polymerization degree generally decreased with the increased in temperature to ensure the reaction temperature was strictly controlled at 25°C. The zeta potential and particle size distribution of CNC were measured using nanometer particle size meter (ZETASIZER NANO ZS, Malvern Panalytical, Ltd., Birmingham, British). The morphology of CNC was observed with a scanning electron microscope (SEM) (ZEISS Sigma 300, Carl Zeiss AG, Oberkochen, Germany) and a digital camera (Canon EOS M50, Tokyo, Japan).

### *2.7. Statistical Analysis*

Word Processing System (WPS) Office software (v2021) was used to calculate the percentages of soluble content, cellulose content, hemicellulose content, lignin content and ash content of different samples and to draw the corresponding bar graphs. SPSS 25.0 software was used for data and variance analysis, and one-way ANOVA was used to test the difference between the contents of each component, where statistical significance was defined as $p < 0.01$. Origin 2021 was used to draw the chemical composition and physical properties in different samples.

## 3. Results and Discussion

### *3.1. Chromosome Number Identification of PML*

Confirming the chromosome ploidy of PML was the first step before comparing PML and MG in this study. Table 1 provides the flow cytometry results of PML and diploid M. lutarioriparius. Significantly, the mean X value and DNA content of PML were 285.5 and 6.3, respectively, which is about 1.5 times of that of diploid M. lutarioriparius. Since the number of chromosomes of diploid M. lutarioriparius is 38 (2×), the number of chromosomes of triploid M. lutarioriparius could be 57 (3×). The result proved that the PML was triploid which was the same for MG. The implication of this result was that all comparisons as shown below removed the effect of ploidy differences between PML and MG.

**Table 1.** Chromosome ploidy of Polyploid *Miscantus lutarioriparius.*

| Species | X-Mean | DNA Content (pg) | Chromosomes Number |
|---|---|---|---|
| Diploid *Miscantus lutarioriparius* | 199.4 | 4.4 | 2n |
| Polyploid *Miscantus lutarioriparius* | 283.5 | 6.3 | 3n |

### *3.2. Significant Differences in Agronomic Traits between PML and MG*

MG, an allotriploid, has been considered as an ideal biomass feedstock for the commercial production of nanocellulose due to high annual biomass yields and cellulose content [31]. In the present study, a natural PML was screened from a nationwide collection, and investigated as a new domesticable and scalable source biomass resource for CNC production, which had exhibited an even higher annual biomass yield than MG in previous study (23.5 vs. 14.1 t/ha) [32].

Apart from annual biomass yield, the employed PML significantly differed from MG in terms of other agronomic traits. Summary statistics of agronomic traits for PML and MG are presented in Figure 1. Compared with MG, PML exhibited higher values in terms of its node number, stem diameter, leaf width and leaf length. By contrast, its values of dry biomass weigh per plant, leaf/stem ratio, panicle height and stem number were lower than MG. Overall, PML is a perennial grass that primarily grows in wetlands along the middle and lower reaches of the Yangtze River, the significant differences in agronomic traits of PML and MG were closely related to their different growth environments and survival strategies [33].

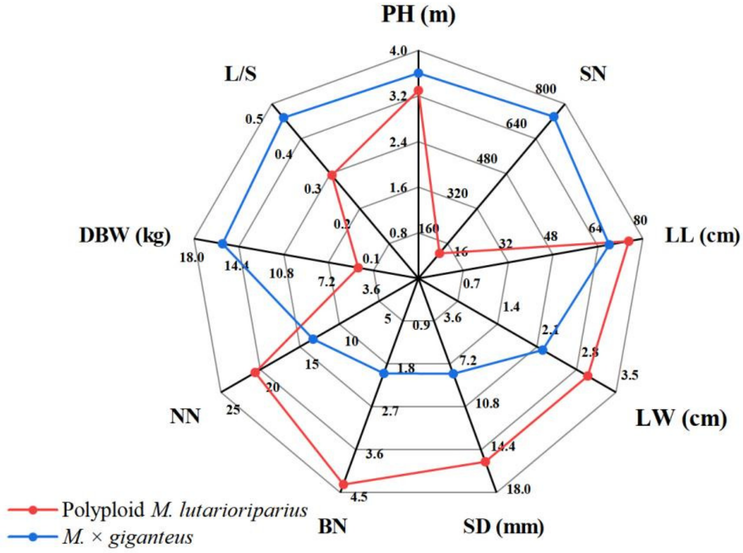


**Figure 1.** Agronomic traits of polyploid *Miscanthus lutarioriparius* and *Miscanthus* × *giganteus*. Dry biomass weight (DBW), leaf/stem ratio (L/S), Panicle height (PH), Stem number (SN), Leaf length (LL), leaf width (LW), stem diameter (SD), Node number (NN).

### *3.3. Comparison of Chemical Components and Physical Features of PML and MG*

The compositional analysis of raw biomass of PML and MG used are presented in Figure 2. The PML raw biomass consisted of 41.0 ± 0.1% cellulose, 22.4 ± 0.3% hemicellulose, 22.0 ± 0.3% lignin, 7.9 ± 0.6% soluble content and 5.3 ± 0.1% ash, so that the lignocellulosic polymers content was over 85.0%. The ANOVA of chemical component contents indicated that there was no significant different between PML and MG. In addition, both PML and MG contained more than 40% cellulose, suggesting a higher potential for nanocellulose production compared with common agricultural wastes (rice straw, wheat straw and corn stalk, etc) and bagasse [34]. Moreover, as the major chemical component inhibiting crude cellulose isolation, the lignin content of PML raw biomass was lower than woody biomass [35]. Meanwhile, the soluble content and ash of PML raw biomass was significantly lower than agricultural waste, indicating its higher utilization rate of raw biomass for biofuel, biomaterials and biochemicals [36].

Since nanocellulose was isolated from the crystalline region of cellulose in plant cell walls, the crystalline index of CrI and DP were considered as the main factors affecting its nanocellulose potential [37]. As shown in Figure 3, the CrI values of the raw biomass of PML and MG were 56.5% and 57.1%, respectively. Additionally, the DP values of the raw biomass of PML and MG were 639 and 618, respectively. Specifically, the CrI and DP values of PML and MG were higher than those of *Miscanthus sinensis*, *Miscanthus floridulus*, *Miscanthus sacchariflorus*, and *Miscanthus lutarioriparius* [30]. Hence, the results indicate that both PML and MG possessed great potential for cellulose derivatives compared to other *Miscanthus* species.

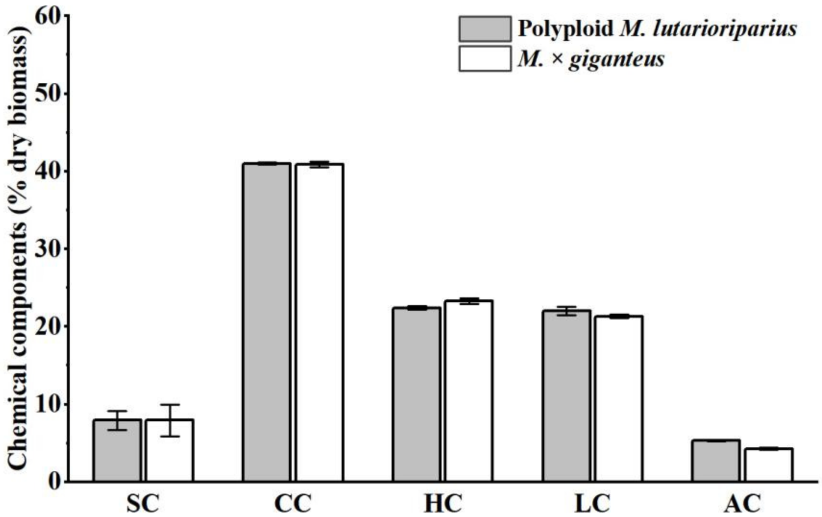


**Figure 2.** Chemical components of lignocellulosic biomass in polyploid *Miscanthus lutarioriparius* and *Miscanthus* × *giganteus*. Soluble content (SC), Cellulose content (CC), Hemicellulose content (HC), Lignin content (LC), Ash content (AC). Vertical bar are standard deviation ($n$ = 2).

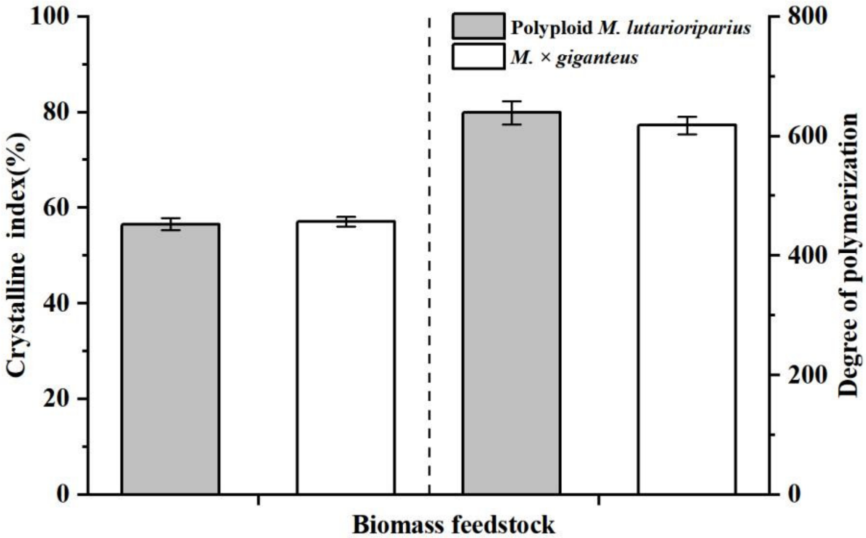


**Figure 3.** Crystalline index and degree of polymerization of lignocellulosic biomass in polyploid *Miscanthus lutarioriparius* and *Miscanthus* × *giganteus*. Vertical bar are standard deviation ($n$ = 3).

### *3.4. Isolation of Crude Cellulose from Raw Biomass of PML and MG by Modified Alkaline Peroxide Pretreatment*

Alkaline peroxide pretreatment has proven to be an excellent method for the separation of crude cellulose from a variety of lignocellulosic biomass [27]. In this study, a modified alkaline peroxide pretreatment was employed to extract crude cellulose from PML and MG. Notably, the cellulose contents of PML and MG increased sharply from 41.0% and 40.9% of raw biomass to 95.9% and 89.9% of crude cellulose, respectively (Figure 4). These results were significantly higher than the cellulose content of crude cellulose extracted from other biomasses by alkaline peroxide pretreatment [27,29]. By contrast, the non-cellulosic polymers (hemicellulose and lignin) of both PML and MG were heavily co-extracted during pretreatment, which could lead to increases in CrI and/or lignocellulose deconstruction [29]. Therefore, the results indicated that the modified alkaline peroxide pretreatment was an effective method by which to isolate crude cellulose from lignocellulose.

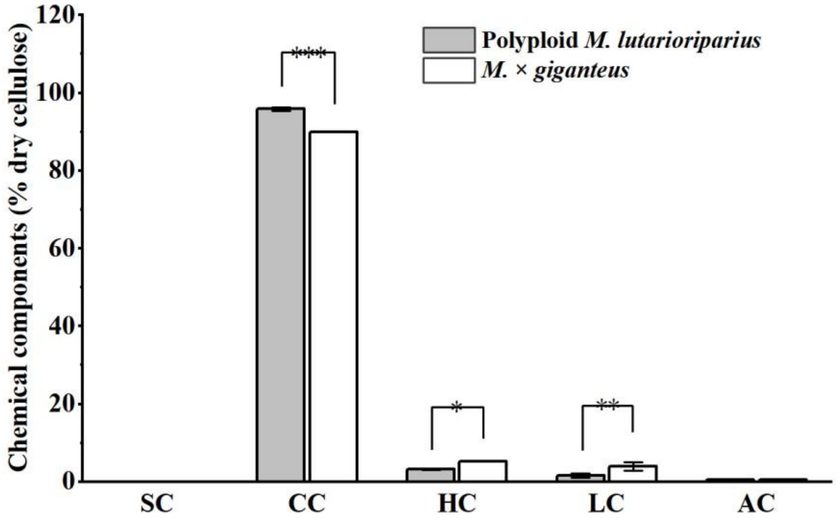


**Figure 4.** Chemical components of crude cellulose in polyploid *Miscanthus lutarioriparius* and *Miscanthus* × *giganteus*. * Significant difference at $p \leq 0.05$, ** Significant difference at $p \leq 0.01$, *** Significant difference at $p \leq 0.001$. Vertical bar are standard deviation ($n$= 2).

To confirm the effects of the isolation process on cellulose structure, the CrI and DP of crude cellulose were detected in this study (Figure 5). Interestingly, the CrI values of crude cellulose extracted from PML (72.4%) and MG (69.8%) were significantly higher than those of their raw biomass, respectively. Meanwhile, the DP values of crude cellulose in PML and MG were less than 1/8 and 1/6 of their raw biomass, respectively. Together, these results provided important insights in that the modified alkaline peroxide pretreatment had exhibited great efficiency in removal of non-cellulosic polymers, as well as the non-crystalline cellulose. Besides, the ideal biomass feedstock of nanocellulose could be identified with high levels of cellulose content, CrI values, low levels of non-cellulosic polymers content and DP values [30,38]. Therefore, the crude cellulose of PML exhibited a greater potential for CNC preparation compared with that of MG.

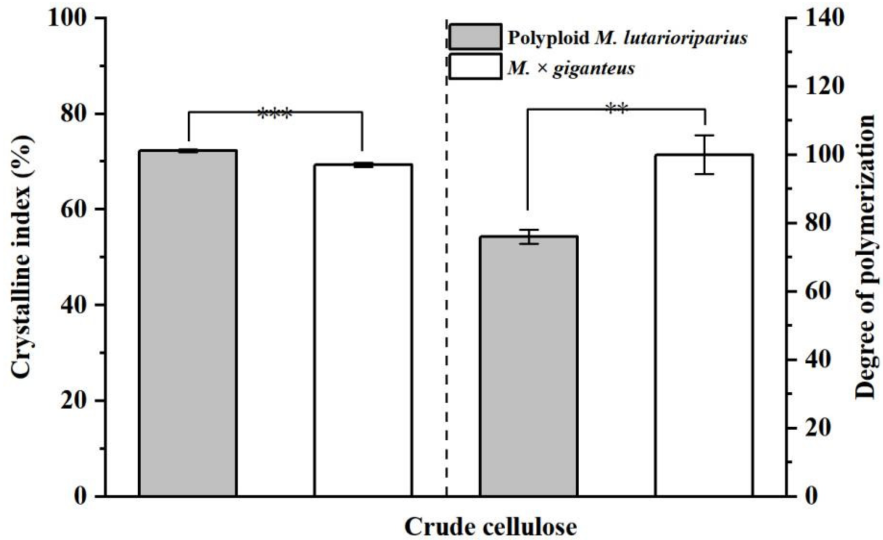


**Figure 5.** Crystalline index and degree of polymerization of crude cellulose in polyploid *Miscanthus lutarioriparius* and *Miscanthus* × *giganteus*. ** Significant difference at $p \leq 0.01$, *** Significant difference at $p \leq 0.001$. Vertical bar are standard deviation ($n$ = 3).

### 3.5. Comparative Analysis of CNC from Crude Cellulose of PML and MG Extracted by Sulfuric Acid Hydrolysis

As the only commercialized technology, sulfuric acid hydrolysis was further applied to isolate CNC from the crude cellulose of PML and MG in this study [39]. Table 2 provides the purity of CNC prepared by PML and MG. Notably, while the CNC purity of MG was slightly lower than that of PML, it was much higher than that of other biomass in previous studies [3,4,6,7,31,34]. Moreover, Figure 6 provides the results obtained from the preliminary analysis of zeta potential and particle size distribution of CNC. Specifically, CNC extracted from PML has a higher zeta potential and more uniform particle size distribution than CNC extracted from MG. Previous studies suggested that the higher the zeta potential of CNC, the more likely the suspension is to be stable as the charged particles repel each other, and this force overcomes the natural tendency to aggregate [40]. In addition, the particle size uniformity of CNC was an important factor affecting their processability to further prepare advanced materials [38]. Hence, the CNC extracted from PML showed higher stability and processability than that from MG.

**Table 2.** The purity of CNCs extracted bisulfuric acid hydrolysis.

| Species | Purity (%) |
|---|---|
| Polyploid *Miscanthus lutarioriparius* | 95.6 |
| *Miscanthus* × *giganteus* | 95.0 |

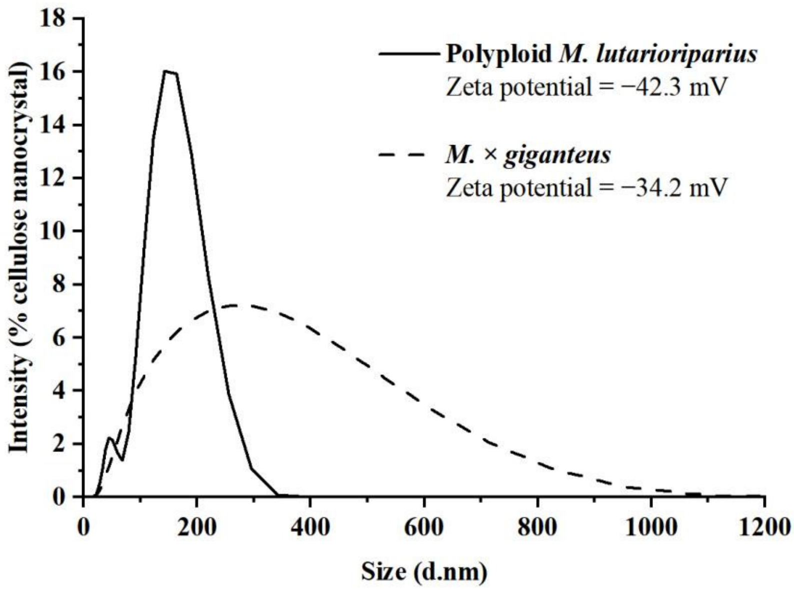


**Figure 6.** Particle size distribution, zeta potential of CNC in polyploid *Miscanthus lutarioriparius* and *Miscanthus* × *giganteus*.

The CrI and DP values of CNC extracted from PML and MG were measured in this study (Figure 7). After sulfuric acid hydrolysis, the CrI values of CNC extracted from PML and MG increased slightly to 75.1% and 74.7%, respectively. The results indicate that the non-cellulose polymers and non-crystalline cellulose were further co-extracted from crude cellulose during the sulfuric acid hydrolysis process, which could lead to improvement of CNC purity. Meanwhile, the DP values of CNC extracted from PML and MG decreased to 56 and 45, respectively. According to the data, we could infer that an internal degradation occurred in the crystalline regions of cellulose during sulfuric acid hydrolysis, which could lead to the further shrinkage of cellulose particles to the nanoscale [41].

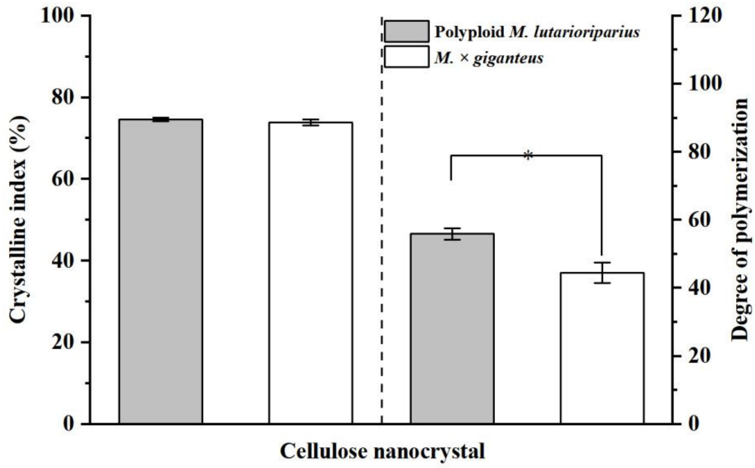


**Figure 7.** Crystalline index and degree of polymerization of CNC in polyploid *Miscanthus lutarioriparius* and *Miscanthus* × *giganteus*.* Significant difference at $p \leq 0.05$. Vertical bar are standard deviation ($n$ = 3).

For an intuitive comparison of the differences in CNC between PML and MG, a series of morphological observations were conducted step by step in the present study. In Figures 8 and 9 an obvious particle size reduction in PML and MG raw biomass is observable after modified alkaline peroxide pretreatment, whereas the color of MG crude cellulose was found to be deeper than that of PML.This result could be explained by the fact that the co-extraction of amorphous substances that occurred in PML raw biomass was more significant than in MG raw biomass, which would theoretically significantly improve the yield and purity of its CNCs (Figures 4, 8D and 9D). The SEM images further confirmed that the CNCs of both PML and MG reached the nanoscale, but their particle shapes were significantly different. To be specific, the CNC of PML exhibited a standard crystal shape, while the CNCs of MG were irregularly shaped and composed of spherical particles (Figure 8). The reason for this is not clear but it may have something to do with the different natural forms of cellulose in PML and MG raw biomass.

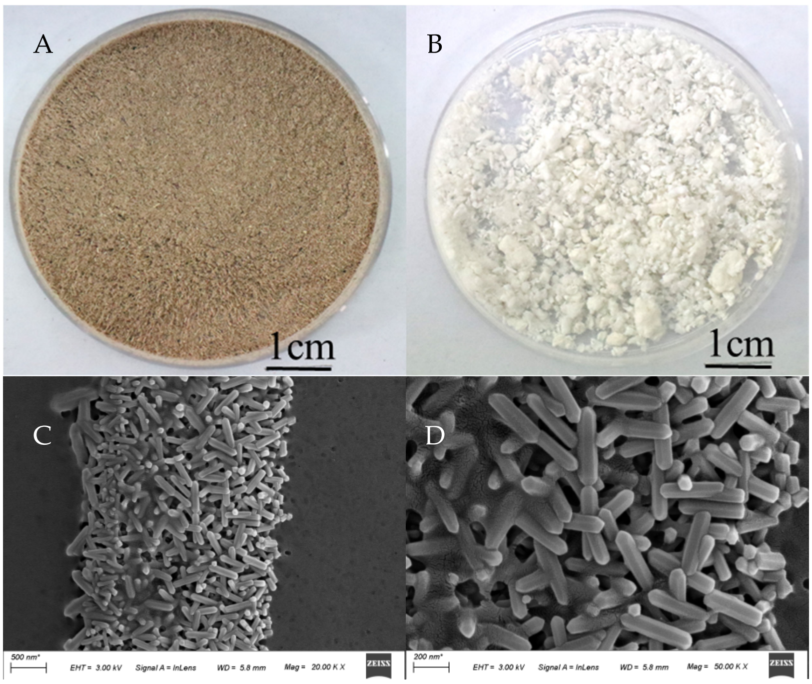


**Figure 8.** Morphological observation of the raw biomass (**A**), crude cellulose (**B**), and the CNC (**C**,**D**) of polyploid *Miscanthus lutarioriparius*.

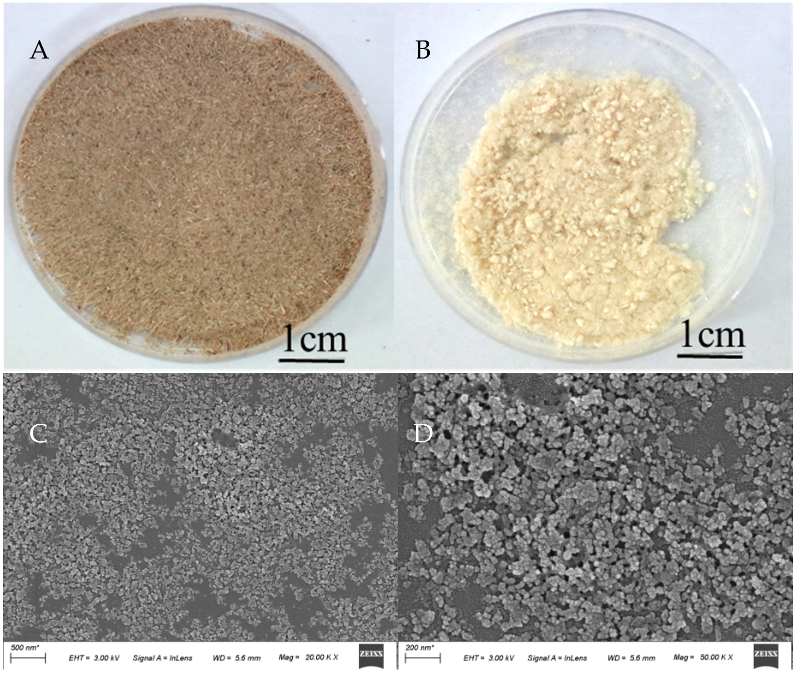


**Figure 9.** Morphological observation of the raw biomass (**A**), crude cellulose (**B**), and the CNC (**C**,**D**) of *Miscanthus* × *giganteus*.

In addition, these CNC, with a regular shape and high crystalline index, have great potential as filler and performance-enhanced materials [4,17]. For example, many polyer (Polylactic acid, xylan, chitosan) complexes with CNC have enhanced mechanical and barrier properties [35,38]. Raghav et al. [3] combined phosphorylated CNCs with drugs to prepare sustained-release carriers [3]. Xie et al. [6] observed an improvement in the tensile strength and oxygen permeability with the addition of CNC to food packaging films.

### *3.6. The Yield Potential of Crude Cellulose and CNC*

Table 3 provides the yield potential of crude cellulose and CNC extraction from PML and MG. Briefly, the crude cellulose yield of PML was slightly lower than that of MG, but its CNC yield was slightly higher than that of MG. A possible explanation for this might be that the CrI values of PML crude cellulose are significantly higher than that of MG crude cellulose, indicating that the content of crystalline cellulose in PML crude cellulose is higher than that in MG crude cellulose (Figure 5). According to our previous study, the dry matter yield of PML and MG were 23.5 t/ha and 14.1 t/ha, respectively [32], which means the 2.4 t and 1.3 t of CNCs can be produced per hectare. Therefore, the results suggested that PML shows greater potential for industrialized CNC preparation compared to MG.

**Table 3.** Yield potential of crude cellulose and CNCs.

| Production | Species | Yield (%, Raw Biomass) |
|---|---|---|
| Crude cellulose | Polyploid *Miscanthus lutarioriparius* | 32.4 |
| Crude cellulose | *Miscanthus* × *giganteus* | 33.7 |
| CNCs | Polyploid *Miscanthus lutarioriparius* | 10.1 |
| CNCs | *Miscanthus* × *giganteus* | 9.9 |

## 4. Conclusions

In this study, a natural autotriploid *Miscanthus lutarioriparius* was firstly and successfully used for CNC preparation via modified alkaline peroxide pretreatment followed by sulfuric acid hydrolysis. Firstly, the agronomic traits of PML were significantly different from those of MG, but their chemical composition and physical features were similar. In addition, a significantly better co-extraction of non-cellulosic polymers and non-crystalline cellulose was obtained by modified alkaline peroxide pretreatment with PML than with MG. As expected, comparative analyses of particle size distribution, zeta potential, CrI, the DP, SEM and yield potential suggest that the CNC extracted from PML showed higher stability, processability and productivity than that from MG. These results provide a new competitive biomass feedstock for CNC preparation and new insight into the integrated utilization of PML for biorefinery.

**Author Contributions:** Conceptualization: S.W. and M.L.; methodology: S.W.; resources: Z.C. and Z.Y.; investigation: Y.I.; data curation, S.W.; writing—original draft preparation, S.W. and M.L.; writing—review and editing S.X. and T.F.; supervision, M.L.; project administration, Z.Y. All authors have read and agreed to the published version of the manuscript.

**Funding:** This research was funded by National Natural Science Foundation of China, (grant number 32000260, 31471557), Natural Science Foundation of Hunan Province (grant number 2020JJ5228), Foundation for the Construction of Innovative Hunan (grant number 2019NK2021), and China Postdoctoral Science Foundation (grant number 2020M682566).

**Institutional Review Board Statement:** Not applicable.

**Informed Consent Statement:** Not applicable.

**Data Availability Statement:** Not applicable.

**Acknowledgments:** We express our deepest gratitude to Hunan Engineering Laboratory of Miscanthus Ecological Applications of Hunan province for providing support and permission to conduct this research. We are thankful to Weiming Liu, Jie Li, Yao Li, Yancen He, Weihong Du and other colleagues for their assistance in data collection.

**Conflicts of Interest:** The authors declare that they have no competing interest.

## References

1. Malherbe, S.; Cloete, T.E. Lignocellulose biodegradation: Fundamentals and applications. *Rev. Environ. Sci. Biotechnol.* **2002**, *1*, 105–114. [CrossRef]
2. Burdick, J.A.; Prestwich, G.D. Hyaluronic Acid Hydrogels for Biomedical Applications. *Adv. Mater.* **2011**, *23*, H41–H56. [CrossRef] [PubMed]
3. Lunardi, V.B.; Soetaredjo, F.E.; Putro, J.N.; Santoso, S.P.; Yuliana, M.; Sunarso, J.; Ju, Y.; Ismadji, S. Nanocelluloses: Sources, Pretreatment, Isolations, Modification, and Its Application as the Drug Carriers. *Polymers* **2021**, *13*, 2052. [CrossRef] [PubMed]
4. Habibi, Y.; Lucia, L.A.; Rojas, O.J. Cellulose nanocrystals: Chemistry, self-assembly, and applications. *Chem. Rev.* **2010**, *110*, 3479–3500. [CrossRef]
5. Tasnim, R.; Calderwood, L.; Tooley, B.; Wang, L.; Zhang, Y. Are Foliar Fertilizers Beneficial to Growth and Yield of Wild Lowbush Blueberries? *Agronomy* **2022**, *12*, 470. [CrossRef]
6. Mateo, S.; Peinado, S.; Morillas-Gutiérrez, F.; La Rubia, M.D.; Moya, A.J. Nanocellulose from Agricultural Wastes: Products and Applications—A Review. *Processes* **2021**, *9*, 1594. [CrossRef]
7. Kargarzadeh, H.; Mariano, M.; Huang, J.; Lin, N.; Ahmad, I.; Dufresne, A.; Thomas, S. Recent developments on nanocellulose reinforced polymer nanocomposites: A review. *Polymer* **2017**, *132*, 368–393. [CrossRef]
8. Lucia, L.A.; Rojas, O.J. Fiber nanotechnology: A new platform for "green" research and technological innovations. *Cellulose* **2007**, *14*, 539–542. [CrossRef]
9. Adelantado, C.; Ríos, Á.; Zougagh, M. Magnetic nanocellulose hybrid nanoparticles and ionic liquid for extraction of neonicotinoid insecticides from milk samples prior to determination by liquid chromatography-mass spectrometry. *Food Addit. Contaminants. Part A Chem. Anal. Control. Expo. Risk Assess.* **2018**, *35*, 1755–1766. [CrossRef]
10. El-Samahy, M.A.; Mohamed, S.A.A.; Rehim, M.H.A.; Mohram, M.E. Synthesis of hybrid paper sheets with enhanced air barrier and antimicrobial properties for food packaging. *Carbohydr. Polym. Sci. Technol. Asp. Ind. Important Polysacch.* **2017**, *168*, 212–219. [CrossRef]
11. Fontenot, K.R.; Edwards, J.V.; Haldane, D.; Pircher, N.; Liebner, F.; Condon, B.D.; Qureshi, H.; Yager, D. Designing cellulosic and nanocellulosic sensors for interface with a protease sequestrant wound-dressing prototype: Implications of material selection for dressing and protease sensor design. *J. Biomater. Appl.* **2017**, *32*, 622–637. [CrossRef] [PubMed]
12. Bacakova, L.; Pajorova, J.; Bacakova, M.; Skogberg, A.; Kallio, P.; Kolarova, K.; Svorcik, V. Versatile Application of Nanocellulose: From Industry to Skin Tissue Engineering and Wound Healing. *Nanomaterials* **2019**, *9*, 164. [CrossRef] [PubMed]
13. Lahiji, R.R.; Xu, X.; Reifenberger, R.; Raman, A.; Rudie, A.; Moon, R.J. Atomic Force Microscopy Characterization of Cellulose Nanocrystals. *Langmuir* **2010**, *26*, 4480–4488. [CrossRef] [PubMed]

14. Chen, Y.; Li, Q.; Li, Y.; Zhang, Q.; Huang, J.; Wu, Q.; Wang, S. Fabrication of Cellulose Nanocrystal-g-Poly(Acrylic Acid-Co-Acrylamide) Aerogels for Efficient Pb(II) Removal. *Polymers* **2020**, *12*, 333. [CrossRef] [PubMed]
15. García, A.; Gandini, A.; Labidi, J.; Belgacem, N.; Bras, J. Industrial and crop wastes: A new source for nanocellulose biorefinery. *Ind. Crops Prod.* **2016**, *93*, 26–38. [CrossRef]
16. Zhang, K.; Sun, P.; Liu, H.; Shang, S.; Song, J.; Wang, D. Extraction and comparison of carboxylated cellulose nanocrystals from bleached sugarcane bagasse pulp using two different oxidation methods. *Carbohydr. Polym.* **2016**, *138*, 237–243. [CrossRef]
17. Barbash, V.A.; Yashchenko, O.V.; Vasylieva, O.A. Preparation and application of nanocellulose from Miscanthus × giganteus to improve the quality of paper for bags. *SN Appl. Sci.* **2020**, *2*, 727. [CrossRef]
18. Atakhanov, A.; Turdikulov, I.; Mamadiyorov, B.; Abdullaeva, N.; Nurgaliev, I.; Khaydar, Y.; Rashidova, S. Isolation of Nanocellulose from Cotton Cellulose and Computer Modeling of Its Structure. *Open J. Polym. Chem.* **2019**, *09*, 117–129. [CrossRef]
19. Li, C.; Liu, G.; Nges, I.A.; Liu, J. Enhanced biomethane production from Miscanthus lutarioriparius using steam explosion pretreatment. *Fuel* **2016**, *179*, 267–273. [CrossRef]
20. Zheng, C.; Iqbal, Y.; Labonte, N.; Sun, G.; Feng, H.; Yi, Z.; Xiao, L. Performance of switchgrass and Miscanthus genotypes on marginal land in the Yellow River Delta. *Ind. Crops Prod.* **2019**, *141*, 111773. [CrossRef]
21. Sai, Y.; Liang, X.; Zuan, W.; Zi-li, Y.I. Principal Components Analysis and Comprehensive Evaluation of Agronomy and Quality Traits of Miscanthus lutarioriparius. *Chin. J. Grassl.* **2016**, *38*, 26–33.
22. Yang, S.; Xue, S.; Kang, W.; Qian, Z.; Yi, Z. Genetic diversity and population structure of Miscanthus lutarioriparius, an endemic plant of China. *PLoS ONE* **2019**, *14*, e211471. [CrossRef] [PubMed]
23. Junyi, D.; Yanlan, S.; Yuhuan, L.; Hongmei, H.; Qingbo, L.; Zili, Y.I.; Zhiyong, C. Characteristics of inorganic salt ion absorption of Miscanthus lutarioriparius polyploid under NaCl stress. *Acta Prataculturae Sin.* **2018**, *35*, 2893–2902.
24. Nguyen, V.T.H.; Kraska, T.; Winkler, W.; Aydinlik, S.; Jackson, B.E.; Pude, R. Primary Mechanical Modification to Improve Performance of Miscanthus as Stand-Alone Growing Substrates. *Agronomy* **2022**, *12*, 420. [CrossRef]
25. Sluiter, A.; Hames, B.; Ruiz, R.; Scarlata, C.; Sluiter, J.; Templeton, D.; Crocker, D. Determination of Structural Carbohydrates and Lignin in Biomass. Available online: https://www.nrel.gov/docs/gen/fy13/42618.pdf (accessed on 18 March 2022).
26. Peng, S.J. The Development of Artificial Polyploid in Miscanthus Lutarioriparius and Its Identification Technique. Master's Thesis, Hunan Agricultural University, Changsha, China, 2016.
27. Gabriel, T.; Belete, A.; Hause, G.; Neubert, R.H.H.; Gebre-Mariam, T. Isolation and Characterization of Cellulose Nanocrystals from Different Lignocellulosic Residues: A Comparative Study. *J. Polym. Environ.* **2021**, *29*, 2964–2977. [CrossRef]
28. Sluiter, A.; Hames, B.; Ruiz, R.; Scarlata, C.; Sluiter, J.; Templeton, D.; Crocker, D. Determination of Ash in Biomass. Available online: https://www.nrel.gov/docs/gen/fy08/42622.pdf (accessed on 18 March 2022).
29. Li, M.; Wang, J.; Yang, Y.; Xie, G. Alkali-based pretreatments distinctively extract lignin and pectin for enhancing biomass saccharification by altering cellulose features in sugar-rich Jerusalem artichoke stem. *Bioresour. Technol.* **2016**, *208*, 31–41. [CrossRef]
30. Zhang, W.; Yi, Z.; Huang, J.; Li, F.; Hao, B.; Li, M.; Hong, S.; Lv, Y.; Sun, W.; Ragauskas, A.; et al. Three lignocellulose features that distinctively affect biomass enzymatic digestibility under NaOH and $H_2SO_4$ pretreatments in Miscanthus. *Bioresour. Technol.* **2013**, *130*, 30–37. [CrossRef]
31. Cudjoe, E.; Hunsen, M.; Xue, Z.; Way, A.E.; Barrios, E.; Olson, R.A.; Hore, M.J.A.; Rowan, S.J. Miscanthus Giganteus: A commercially viable sustainable source of cellulose nanocrystals. *Carbohydr. Polym.* **2017**, *155*, 230–241. [CrossRef]
32. Xiang, W.; Xue, S.; Qin, S.; Xiao, L.; Liu, F.; Yi, Z. Development of a multi-criteria decision making model for evaluating the energy potential of Miscanthus germplasms for bioenergy production. *Ind. Crops Prod.* **2018**, *125*, 602–615. [CrossRef]
33. Yan, J.; Chen, W.; Luo, F.; Ma, H.; Meng, A.; Li, X.; Zhu, M.; Li, S.; Zhou, H.; Zhu, W.; et al. Variability and adaptability of Miscanthus species evaluated for energy crop domestication. *Glob. Change Biol. Bioenergy* **2012**, *4*, 49–60. [CrossRef]
34. Yang, H.; Zhang, Y.; Kato, R.; Rowan, S.J. Preparation of cellulose nanofibers from Miscanthus x. Giganteus by ammonium persulfate oxidation. *Carbohydr. Polym.* **2019**, *212*, 30–39. [CrossRef] [PubMed]
35. Lee, H.V.; Hamid, S.B.A.; Zain, S.K. Conversion of Lignocellulosic Biomass to Nanocellulose: Structure and Chemical Process. *Sci. World J.* **2014**, *2014*, 1–20.
36. Brosse, N.; Dufour, A.; Meng, X.; Sun, Q.; Ragauskas, A. Miscanthus: A fast-growing crop for biofuels and chemicals production. *Biofuels Bioprod. Biorefining* **2012**, *6*, 580–598. [CrossRef]
37. Sharma, A.; Thakur, M.; Bhattacharya, M.; Mandal, T.; Goswami, S. Commercial application of cellulose nano-composites—A review. *Biotechnol. Rep.* **2019**, *21*, e00316. [CrossRef]
38. Brinchi, L.; Cotana, F.; Fortunati, E.; Kenny, J.M. Production of nanocrystalline cellulose from lignocellulosic biomass: Technology and applications. *Carbohydr. Polym.* **2013**, *94*, 154–169. [CrossRef]
39. Jonoobi, M.; Oladi, R.; Davoudpour, Y.; Oksman, K.; Dufresne, A.; Hamzeh, Y.; Davoodi, R. Different preparation methods and properties of nanostructured cellulose from various natural resources and residues: A review. *Cellulose* **2015**, *22*, 935–969. [CrossRef]
40. Thomas, B.; Raj, M.C.; Athira, K.B.; Rubiyah, M.H.; Sanchez, C. Nanocellulose, a Versatile Green Platform: From Biosources to Materials and Their Applications. *Chem. Rev.* **2018**, *118*, 24. [CrossRef]
41. Ribeiro, R.; Pohlmann, B.C.; Calado, V.; Bojorge, N.; Pereira, N. Production of nanocellulose by enzymatic hydrolysis: Trends and challenges. *Eng. Life Sci.* **2019**, *19*, 279–291. [CrossRef]